Journal of MATERIALS RESEARCH

Invited Paper
DOI:10.1557/s43578-020-00096-z

ADVANCED NANOMECHANICAL TESTING

FOCUS ISSUE

# Dislocation–grain boundary interactions: recent advances on the underlying mechanisms studied via nanoindentation testing

Farhan Javaid[1,2], Habib Pouriayevali[1], Karsten Durst[1,a)]

[1] Physical Metallurgy Division, Materials Science Department, Technische Universität Darmstadt, Darmstadt, Germany
[2] School of Chemical & Materials Engineering (SCME), National University of Sciences & Technology (NUST), H-12, Islamabad 44000, Pakistan
[a)] Address all correspondence to this author. e-mail: k.durst@phm.tu-darmstadt.de

Received: 16 November 2020; accepted: 22 December 2020; published online: 19 January 2021

**To comprehend the mechanical behavior of a polycrystalline material, an in-depth analysis of individual grain boundary (GB) and dislocation interactions is of prime importance. In the past decade, nanoindentation emerged as a powerful tool to study the local mechanical response in the vicinity of the GB. The improved instrumentation and test protocols allow to capture various GB–dislocation interactions during the nanoindentation in the form of strain bursts on the load–displacement curve. Moreover, the interaction of the plastic zone with the GB provides important insight into the dislocation transmission effects of distinct grain boundaries. Of great importance for the analysis and interpretation of the observed effects are microstructural investigations and computational approaches. This review paper focused on recent advances in the dislocation–GB interactions and underlying mechanisms studied via nanoindentation, which includes GB pop-in phenomenon, localized grain movement under ambient conditions, and an analysis of the slip transfer mechanism using theoretical treatments and simulations.**

## Introduction

The plastic behavior of metals is mainly governed by the motion of dislocations, whereas in polycrystalline materials, dislocation–grain boundary (GB) interactions strongly impact the mechanical response [1–10]. Grain boundaries are often considered to act as a stationary impediment to the dislocation motion, which substantially increases the yield strength of the polycrystalline materials due to dislocations pile-ups in the vicinity of the GB. According to the well-known Hall–Petch relationship [2], the yield strength of the polycrystalline material increases with decreasing the grain size, which also gave rise to the notion "smaller is stronger".

Grain boundaries are not alike and have a different character. However, the classical Hall–Petch model considered only an average hardening contribution by treating all GBs the same. To precisely predict the mechanical behavior of a polycrystalline material at a local scale, a quantitative understanding of the contribution of the individual GB character on the dislocation grain boundary interaction is required [11–13]. Depending upon the GB character, type of dislocations, grain orientation of the adjacent grains, and loading conditions, various interactions between dislocations and individual GB have been reported [14, 15].

i. Dislocations can pile-up or stored at the GB.
ii. Dislocations can be absorbed in the GB (without transmission of dislocations in adjacent or parent grain).
iii. Dislocations can be transmitted in the adjacent grain, with or without leaving a residual dislocation in the GB.
iv. Absorbed dislocations at the GB can be re-emitted in the adjacent grain with or without leaving a partial dislocation in the GB.

v. Absorbed dislocations at the GB can return to the parent grain with or without leaving a partial dislocation in the GB.

Depending upon the adjacent grain orientation, GB character, and the nature of the dislocations, among the above-mentioned dislocations–GB interactions, one or more events can occur at the same time [16–20]. However, due to the complex GB structure and evolving boundary conditions of the adjacent grains during the plastic deformation, reliable criteria for various dislocations–GB interactions are still missing [21].

In the literature, theoretical descriptions and numerical simulation of the interaction between dislocations and GBs have been attempted for a wide range of observation scales. In this regard, different methods like molecular dynamics simulations, discrete dislocation dynamics theories, and continuum crystal plasticity frameworks have been employed [22–27]. Moreover, slip transmission criteria at GBs have been formulated, which consider the misalignment between directional flows at the grains adjacent to a GB as well as the misorientation between slip directions and the normal of GB plane [15, 28–31]. Conventional continuum-scale frameworks are not capable of formulating the microforces imposed by a dislocation pile-up at the GB. Therefore, strain gradient crystal plasticity theories with the potential of incorporating a description of geometrically necessary dislocations (GNDs) have been recently developed [32–35].

To understand the underlying dislocation–GB mechanisms, a range of experimental approaches has been utilized. For example, the slip transfer across the GBs in bulk samples has been investigated via Tensile Testing Setup along with X-ray diffraction [36–38] and Scanning Election Microscopy (SEM) [39–42]. Digital image correlation combined with SEM has been used to investigate the strain along with slip transfer across the GBs [43–45]. The strain accumulation in the vicinity of the GBs also been studied via Electron Backscattered Diffraction (EBSD) [46–48]. To study the GB–dislocation interactions at the atomic scale, Transmission Electron Microscopy (TEM) has been utilized in the literature [14, 49–51]. A small dimension specimen's mechanical response is different as compared to the bulk material. Therefore, over the past decade, the micropillar compression (ranging from micron to sub-micron diameter) testing has gained significant interest [52–57]. The micropillar compression testing experiments have also been conducted to study the individual GB–dislocation interaction. These studies are mostly conducted on the face-centered cubic (FCC) metals [54, 58–61]. However, the first body-centered cubic (BCC) bicrystal pillar compression testing was reported recently [62], in which the micropillar compression testing was conducted on nominally 8 μm diameter Tantalum bicrystal and the slip transmission across three high-angle GBs is investigated.

Over the last decade, substantial advances in the nanoindentation (also known as instrumented or depth-sensing indentation) systems and new test protocols have opened new directions to study the small-scale mechanical properties [63–65]. For example, fast time constant (10's of μs) and high data acquisition rates (close to MHz) [66] allow to capture various events (e.g., slip transmission across the GB [67–70], phase transformation [71, 72], cracking [73–76], etc.) during nanoindentation in the form of strain bursts in the load–displacement curve. The steady advancement in the nanoindentation systems along with data analysis protocols made it a powerful tool to study the local mechanical response in the grain interior [77–81] and the vicinity of the individual GB [67–69, 82].

Nanoindentation combined with advanced characterization techniques [like EBSD, Electron Channeling Contrast Imaging (ECCI), TEM, etc.] and simulations will lead to a better understanding of the underlying mechanisms of the individual GB–dislocation interactions, which is the main focus of the present review paper. The paper includes GB pop-in phenomenon ("GB pop-in phenomenon" section), localized grain movement under ambient conditions ("Stress-driven GB movement during indentation under ambient), and an analysis of the slip transfer mechanism using theoretical treatments and simulations ("Theoretical and numerical concepts for slip transfer" section).

## Dislocations–grain boundary interactions studied via indentation

### GB pop-in phenomenon

In nanoindentation testing, load on the indenter tip and displacement of the indenter tip into the material surface are continuously measured in real time. The load–displacement (LD) curve obtained from nanoindentation tests often shows displacement bursts, which are referred to as "pop-ins" (schematically shown in Figs. 1 and 2). The initial contact is elastic in nature and the first pop-in (Fig. 1b) observed at low load levels often depicts the elastic to the plastic transition of the material. At the pop-in dislocations that are nucleated and afterward, the material deforms elastic-plastically [83–86]. The stress required for the activation of dislocation sources depends on the dislocation density within the stressed region. Specifically, if the test specimen is not well prepared or has been pre-deformed, even for the same material, the initial pop-in load can vary strongly [76, 87]. Ohmura et al. [88] reported that the indentations conducted in the grain interior show the initial pop-in at a relatively larger load as compared to the indentation performed close to the GB. In this work, the authors proposed that the GBs can be an effective source of dislocations which results in the smaller initial pop-in load and size.

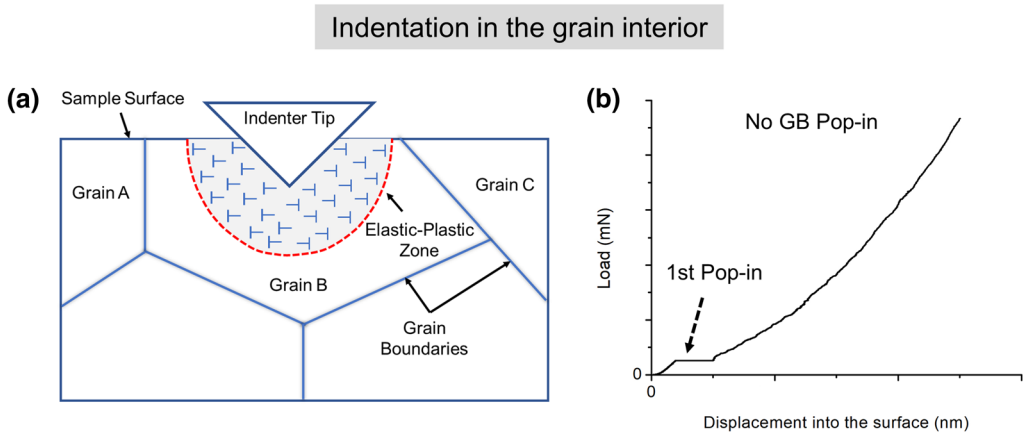


**Figure 1:** Schematic diagram of (a) an indentation performed in the grain interior, (b) LD curve showing only initial pop-in event.

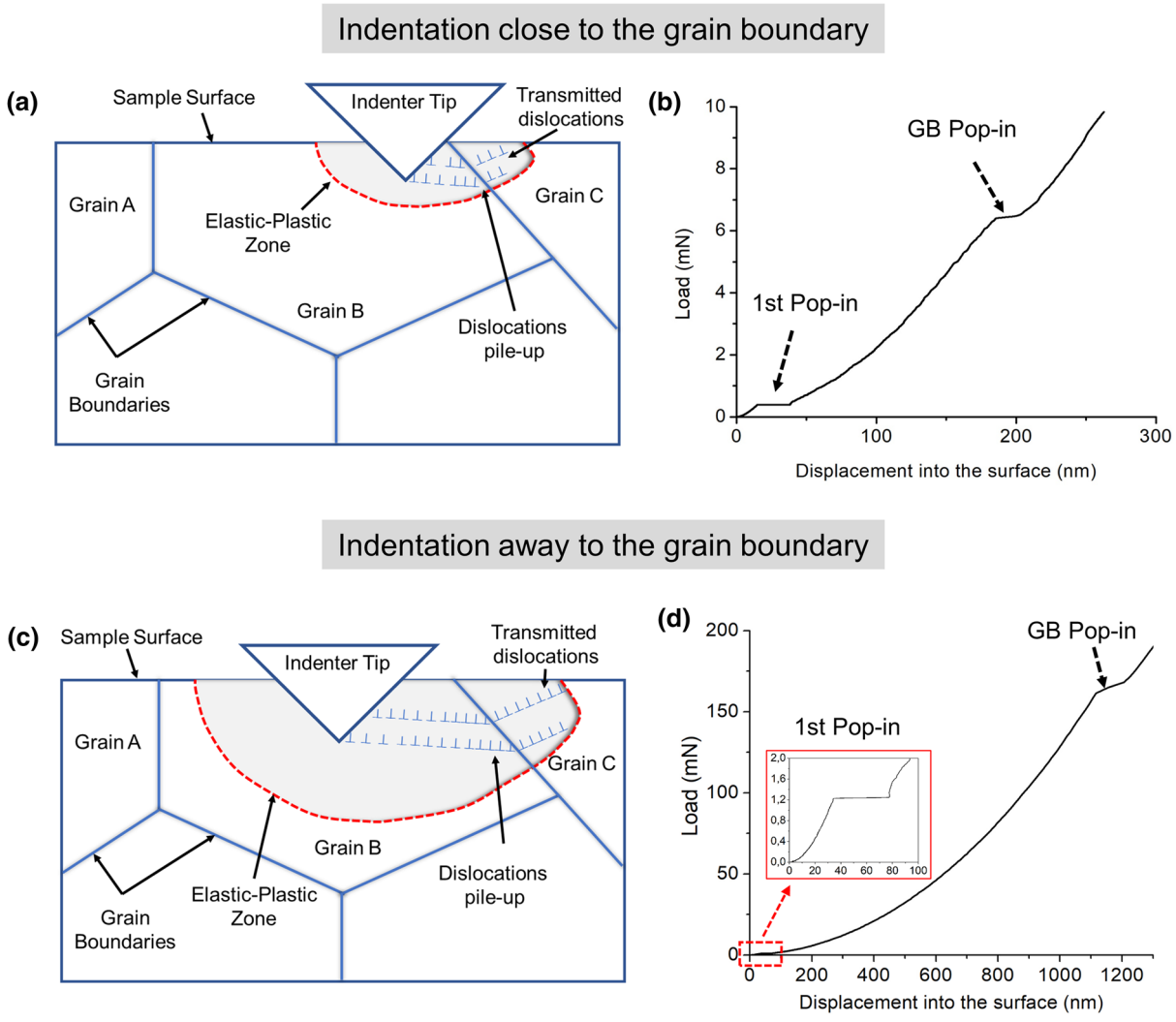


**Figure 2:** Schematic diagram of (a) an indentation performed very close to the GB, (b) representative LD curve of the indentation (a) showing GB pop-in at smaller load, (c) the indentation performed at a larger distance to the GB, and (d) representative LD curve of the indentation (c) showing GB pop-in at relatively higher load.

For the indentations performed in the grain interior, along with the first pop-in, often multiple secondary pop-ins at relatively higher loads have been reported on the LD curve. Such multiple pop-ins are possibly due to further activation of dislocation activity in the expanding plastic zone or other effects like cracking or phase transformation of material during indentation, as has been briefly mentioned in the introduction part.

If the indentation is performed close to the GB, in addition to the first pop-in, a single [70] or multiple secondary pop-ins [89] at relatively higher loads have been observed on the LD curve. These secondary pop-ins are related to the dislocation–grain boundary interactions and are referred to as "GB pop-ins".

The occurrence of the GB pop-in events is strongly influenced by the applied load, the distance of the indenter tip to the GB, misorientation between the adjacent grains, GB character, and the orientation of the indenter tip with respect to the GB [67–70, 82]. The influence of the distance of the indenter tip to the GB on the occurrence of the GB pop-in loads is schematically shown in Fig. 2. In Fig. 2, two cases for the occurrence of the GB pop-in events are schematically presented, assuming that only the distance between the indenter and the grain boundary is varied between Fig. 2a and c. The misorientation between the adjacent grains (grains B and C), GB character (GB between grains B and C), and the orientation of the indenter tip with respect to the GB is thus assumed to be the same. In the first case, the indentation is conducted very close to the GB, in grain B (Fig. 2a). In the second case, the indentation is performed at a much larger distance to the same GB, in grain B (Fig. 2c). Due to the larger indenter tip distance to the GB, dislocations need to travel more distance to reach the GB and then pile-up in the vicinity of the GB. After the critical stress is reached, the dislocations will transmit to the adjacent grain C and the GB pop-in event can occur at a much larger load (schematically shown in Fig. 2d) as compared to the indentation performed very close to the GB (Fig. 2b). It is also clear from the schematic Fig. 2a and c that the elastic–plastic zone below the indentation is much larger for the indentation performed far away from the GB as compared to the indentation performed very close to the GB.

Up to date, experimental observations of the GB pop-in have only been reported for BCC materials like Fe–0.01 wt% C [68], Fe–2.2 wt% Si [90], Fe–14 wt% Si [69, 89], Molybdenum [82, 89, 91], Tungsten [9, 70], Niobium [67], and the intermetallic $L_{12}$ phase $Ni_3Al$ [92]. Due to the lower Hall–Petch constant, in FCC metals, it is suggested that slip transfer phenomena are relatively easier as compared to BCC metals [67]. It seems that in BCC metals, other than FCC metals, slip transfer across the GB requires relatively high local stresses. The slip transfer causes then a relaxation of these stresses, which manifests itself in a GB pop-in and this is one possible reason, why GB pop-ins are mainly reported in BCC materials. Moreover, a GB hardening effect has been found showing an increasing hardness with a decreasing distance to the GB. However, there has been recently some debate in the literature on the GB hardening effect. Wo and Ngan [92] studies on $Ni_3Al$ and Soer et al.[69] on Fe–14 wt% Si bicrystal did not observe appreciable GB hardening, while in another Fe–14 wt% Si [89] investigation, Soer et al. reported the GB hardening effect. Moreover, Wang and Ngan [67] work on niobium, Britton et al. [68] on Fe–0.01 wt% C, and recently Javaid et al. [9, 70] on tungsten clearly show a significant increase in hardness before the GB pop-in events. The absence of GB hardening effect in $Ni_3Al$ [92] and Fe–14 wt% Si [69] could be related to the GB type or the used experimental conditions, so further clarification is required.

Wang and Ngan [67] also proposed a criterion for the occurrence of the GB pop-in events, based on an analysis of the size of the plastic zone with respect to the distance to the GB, the $c/d$-ratio. Here, $c$ is the radius of the elastic–plastic boundary when the strain burst occurs, and $d$ is the distance from the center of residual impression to the GB. They reported a $c/d$-ratio between 1.5 and 5 for various GBs and suggested that for a specific GB, this range should be narrow. Britton et al. [68] and Javaid et al. [70] also validated this criterion and found the $c/d$-ratio to be 1.2 and 1.6–2.7, respectively. Obviously, dislocations need to reach the grain boundary and local stresses require to rise in order to initiate a grain boundary pop-in event. The conditions for the occurrence of a GB pop-in will thereby strongly depend on the local stress state, which again can depend on additional parameters (like GB structure, indenter tip, inclination of the GB below the surface, indentation size effect, etc.) not considered in the $c/d$-ratio.

The GB pop-in events are believed to be associated with the dislocation transmission across the GB. The possible mechanism for such dislocation–GB interaction is that during the indentation process, dislocations are generated around and below the indentations. These dislocations travel toward the GB and form pile-up in the vicinity of the GB. Some dislocations may also be absorbed by the GB. On further loading, a critical stress will reach at which these absorbed, and pile-up dislocations transfer to the adjacent grain which leads to a sudden displacement burst (GB pop-in) on the LD curve. On the basis of in situ straining TEM observations [93], some studies [67–69, 94] believed that the dislocations absorption at the GB and their re-emission is the possible mechanism for the GB pop-in event. However, no direct experimental evidence of the linkage of the GB pop-in event with the absorption of the dislocation at GB and their re-emission has been reported in the literature.

Recently, Javaid et al. [70] reported a statistical analysis on the GB pop-in events in the coarse grain polycrystalline tungsten and also studied the three-dimensional dislocation structure at the GB pop-in events using a combination of sequential polishing and ECCI technique. They confirm that

all set of Berkovich indentations performed in the vicinity of an individual GB (with misorientation of 57° between the adjacent grain) show the GB pop-ins. Javaid et al. [70] also confirm that at the GB pop-in events, the residual impressions were not touching the GB, which discarded the physical contact between indenter and GB as a possible mechanism for the occurrence of the GB pop-in. They stopped the indentations at the GB pop-in events and obtained various cross-sections using a sequential polishing technique [95]. The ECCI images on the sequential polished obtained cross-section clearly show the dislocation pile-up and transmission in the vicinity of the GB at the GB pop-in events. An exemplary image from this work is shown in Fig. 3.

In this three-dimensional investigation, Javaid et al. [70] also reported that Berkovich indenter tip orientation with respect to the GB strongly influenced the content of dislocation traveling toward the GB and transmitted in the adjacent grain. From the three-dimensional analysis, they clearly show that when the side of the Berkovich indenter was facing the GB, more dislocation content was observed near the GB in both grain A and B (shown in Fig. 3) as compared to the indenter tip facing the GB. They also relate the observed high transmitted dislocation content with the measured hardness values before the GB pop-in events. When the Berkovich indenter side was facing the GB, they observed higher transmitted dislocation in the adjacent grain (Fig. 3) as well as higher hardness values before the GB pop-in event as compared to the indentations where the Berkovich indenter tip was facing the GB. Recently, Jakob et al. [82] also reported that the orientation of the Berkovich indenter tip with respect to the same GB can strongly influence the measured hardness values.

To validate the linkage between the occurrence of the GB pop-in event with the absorption of dislocation at GB and their re-emission as the possible mechanism, further in situ nanoindentation and computational studies are required.

## Stress-driven GB movement during indentation under ambient conditions

Under ambient conditions, GBs are considered as obstacles to the dislocation motion in the coarse grain (> 1 μm) polycrystalline metals. The well-known Hall–Petch relation is based upon this assumption. Recent studies [83, 96–102] on nanocrystalline materials suggest that the GBs cannot always be considered as static structures under ambient conditions. Such localized GB migration cannot be explained by using classical grain growth models [103] and, therefore, are distinguished as the stress-driven GB movement. Since the present review is largely focused on the indentation-based dislocation–GB interactions, only indentation studies revealing the localized GB movement will be reviewed in the preceding paragraph.

The stress-driven GB movement has been observed mostly in the ultrafine grain FCC metallic materials. For example, Minor et al. [83] performed the in situ TEM indentation experiments on the ultrafine grain aluminum (Al) and observed a significant GB movement at room temperature. They suggested that the inhomogeneous stress field below the indentation can possibly lead to such a localized stress-driven GB movement. Later, Soer et al. [104] also conducted similar experiments on

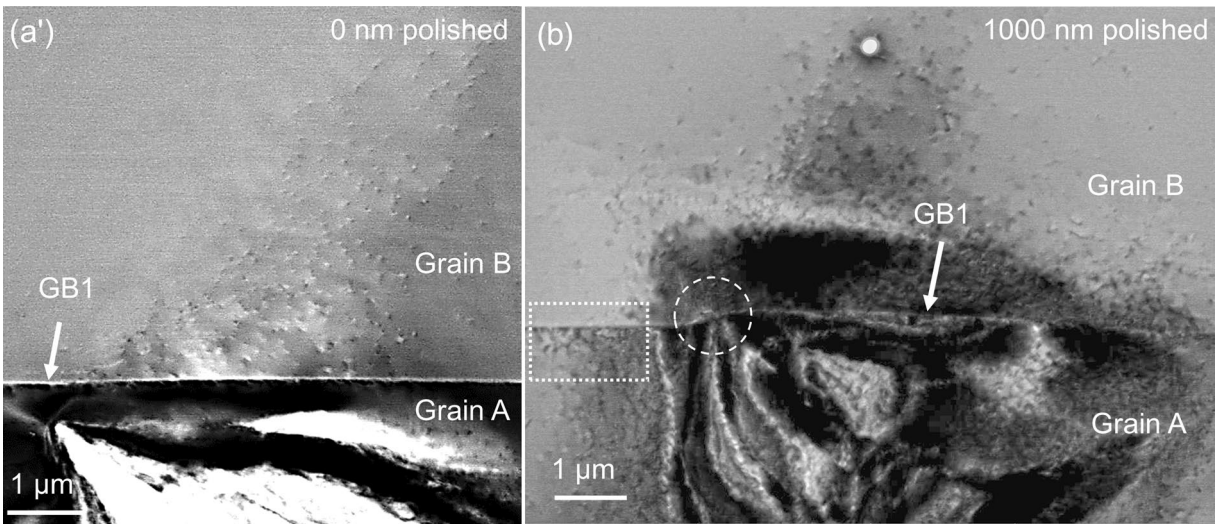


**Figure 3:** ECCI images of the indent (one side facing GB), (a) at the surface along, with inset region (b) showing dislocation pile-up in grain A (rectangular dotted area) and transmitted dislocation in grain A and B at—1000 nm [70].

the ultrafine grain Al and validated the extensive stress-driven GB motion from in situ TEM studies. In the same work, they also studied the aluminum–magnesium (Mg) alloy thin films via in situ TEM studies and observed that the high-angle GBs are effectively pinned by Mg solutes, whereas the low-angle GBs remained unaffected by the Mg solutes. The stress-driven GB movement is also demonstrated as grain growth in ultrafine grain Al thin films [96, 97]. Zhang et al. [98] conducted the in situ TEM indentation studies on nanocrystalline copper at ambient and cryogenic temperatures and observed rapid stress-driven grain coarsening below the indentation. Moreover, they observed that the grain coarsening under the inhomogeneous stress field was even faster at cryogenic temperature as compared to the ambient conditions.

Interestingly, all aforementioned stress-driven GB movement studies are conducted on ultrafine grained FCC metals and alloys. Recently, Javaid et al. [9] conducted the ex situ Berkovich nanoindentation experiments close to the different GBs of coarse-grained polycrystalline BCC tungsten. For multiple Berkovich indentations, they observed a significant localized GB movement inside the residual impression as well as below the indentation in the plastic zone (Fig. 4).

From their experimental observations, the authors differentiate three cases. In 1st case (Fig. 4a and d), no grain boundary movement is observed inside or below the indentation. In 2nd case, a significant grain boundary movement (indicated by XX*) is visible inside the residual impression (Fig. 4b) on the surface. However, below the indentation, the grain boundary becomes straight again (Fig. 4e). In the 3rd case, no grain boundary movement is noticeable inside the indentation (Fig. 4c) on the surface. The sequential polishing, however, revealed a clear grain boundary curvature (indicated by YY*) below the indentation (Fig. 4f). The driving force for such a localized grain boundary movement is believed to be high local dislocation density in the vicinity of the grain boundary. They also reported that the localized GB movement in tungsten is strongly influenced by the misorientation between the adjacent grain, distance of the indenter to the GB, the orientation of Berkovich indenter with respect to GB, and the applied load.

The stress-driven GB movement during indentation arises from the inhomogeneous stress field which leads to complex dislocation–GB interactions, which are not so easy to model. Cahn and Taylor [105, 106] proposed a unified theory of coupled GB motion, which shows reasonable agreement with the experimental work of Winning et al. [107, 108] performed on the Al bicrystal and also with Molecular Dynamics Simulations [106, 109]. However, to understand the underlying mechanisms during indentation-induced GB motion in detail, comprehensive three-dimensional in situ nanoindentation experiments along with modeling effort are further required.

## Theoretical and numerical concepts for slip transfer

It is well accepted that misalignments at grain boundaries affect the ease of dislocation transmission. Therefore, geometric criteria, which take into account the misalignment between slip

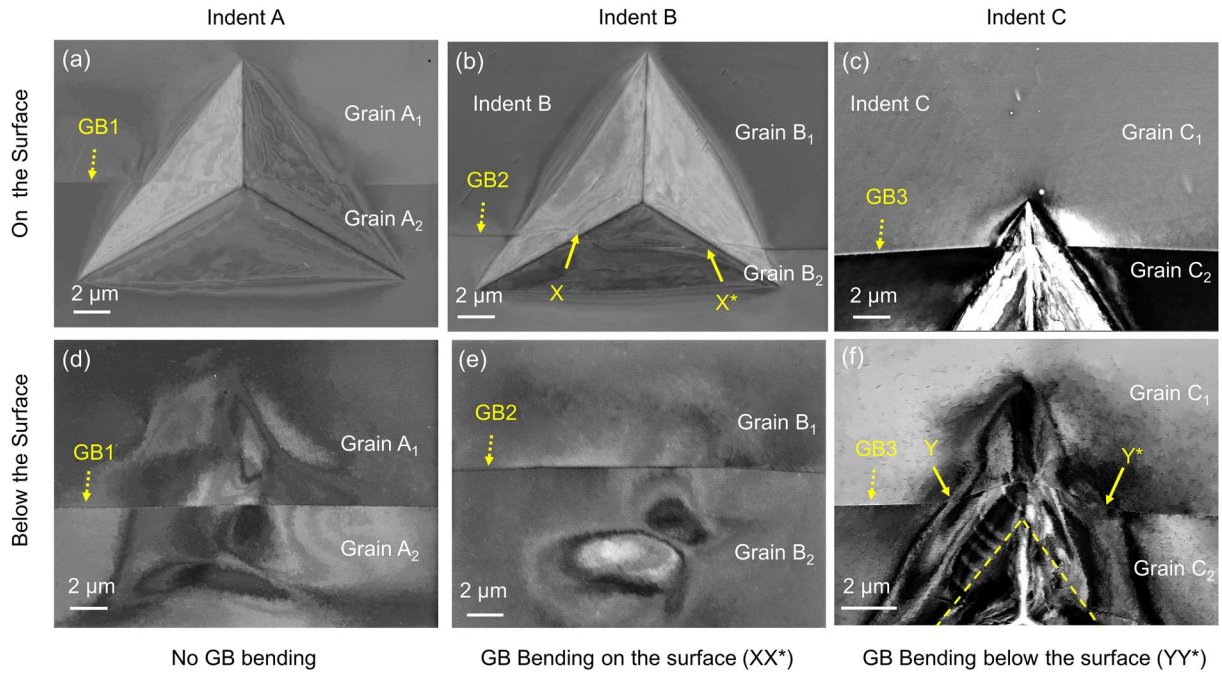


**Figure 4:** SEM and ECCI images of representative 2-μm-deep Berkovich indentations (a–c) on the surface and (d–f) below the surface obtained from sequential polishing [adapted with permission from Ref. [9].

systems on both sides of a GB as well as the misorientation between the GB plane and slip systems, have been formulated. In the following, those slip transfer criteria are briefly discussed, see also Fig. 5. One of the earliest formulations were proposed in [28] as follows:

$$\tau_\beta = N^{\beta\alpha}\tau_\alpha, N^{\beta\alpha} = \left(\boldsymbol{m}_{\mathrm{B}}^{\beta}\cdot\boldsymbol{m}_{\mathrm{A}}^{\alpha}\right)\left(\boldsymbol{s}_{\mathrm{B}}^{\beta}\cdot\boldsymbol{s}_{\mathrm{A}}^{\alpha}\right)+\left(\boldsymbol{m}_{\mathrm{B}}^{\beta}\cdot\boldsymbol{s}_{\mathrm{A}}^{\alpha}\right)\left(\boldsymbol{s}_{\mathrm{B}}^{\beta}\cdot\boldsymbol{m}_{\mathrm{A}}^{\alpha}\right), \tag{1}$$

where the unit vectors $\boldsymbol{m}$ and $\boldsymbol{s}$ denote the normal vector of slip plane and the slip direction, respectively, and $\alpha$ and $\beta$ stand for slip system numbers (Fig. 5). The resultant shear stress $\tau_\beta$ on the slip system $\beta$ in the crystal B is here related to the counterpart shear stress $\tau_\alpha$ on the slip system $\alpha$ in the crystal A. Considering the slip system $\alpha$ incoming toward the grain boundary, the outgoing slip system $\beta$ is most probably activated when the associated factor $N^{\beta\alpha}$ is high enough. Here, the interaction factor $N^{\beta\alpha}$ is independent of the boundary inclination. It is worth noting that the contribution of the aforementioned factor needs in-depth discussions. As an example, when two slip planes on the sides of a GB are parallel to the GB plane, $N^{\beta\alpha}$ might equal to 1, however, if one of these slip planes becomes perpendicular to another one, $N^{\beta\alpha}$ could again yield 1 which leads to an unphysical interpretation.

Later, Luster and Morris [110] introduced a geometric compatibility factor $m'$ by dropping the second term on the right side of Eq. (1).

$$m' = \left(\boldsymbol{m}_{\mathrm{B}}^{\beta}\cdot\boldsymbol{m}_{\mathrm{A}}^{\alpha}\right)\left(\boldsymbol{s}_{\mathrm{B}}^{\beta}\cdot\boldsymbol{s}_{\mathrm{A}}^{\alpha}\right) = \cos\phi\cdot\cos\kappa, \tag{2}$$

where $\phi$ is the angle between slip plane normals and $\kappa$ is the angle between incoming and outgoing slip directions, which are illustrated in Fig. 5. Here, no contribution of grain boundary inclination is again seen. In a study of annealed polycrystalline Al foils with near-cube oriented grains [111], it was found that the slip transfer across GBs is very rare and is only evident when $m' > 0.97$. Moreover, a study of the slip transfer in Ti-6Al-4 V [112] shows that slip transfers might occur in a wider range of $m'$ values when applied stresses increase, Fig. 6 in [112]. Performing the nanoindentation at the area of GBs in a polycrystalline niobium [67] indicates that the GB pop-in might be seen within the maximum load of 50 mN, when $m' > 0.93$. In a study of the correlation between intragranular slip transmissions and the GB misorientation in a polycrystalline $Ni_3Al$ [92], good concurrences were found between the ease of transmission and high values of $m'$ as well as between the difficulty in the transmission and $m' \leq 0.96$.

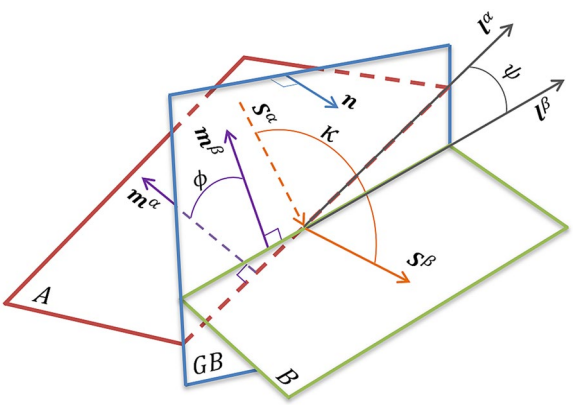


**Figure 5:** Two slip planes A and B adjacent to a grain boundary (GB) plane. $\boldsymbol{m}$ and $\boldsymbol{s}$ denote the normal vector of the slip plane and the slip direction, respectively. $\alpha$ and $\beta$ stand for slip system numbers. $\boldsymbol{l}$ is the unit vector at the intersection line and $\boldsymbol{n}$ is the normal vector of grain boundary plane. Three angles $\phi$, $\psi$, *and* $\kappa$ depict the misorientation at the GB.

Considering the role of grain boundary orientation, Shen et al. [29] proposed a modified geometric criterion accounting for the misorientation of intersection lines and slip directions as follows:

$$K^{\alpha\beta} = \left(\boldsymbol{l}_{\mathrm{A}}^{\alpha}\cdot\boldsymbol{l}_{\mathrm{B}}^{\beta}\right)\left(\boldsymbol{s}_{\mathrm{A}}^{\alpha}\cdot\boldsymbol{s}_{\mathrm{B}}^{\beta}\right) = \cos\psi\cdot\cos\kappa, \boldsymbol{l}_{\mathrm{A}}^{\alpha} = \boldsymbol{m}_{\mathrm{A}}^{\alpha}\times\boldsymbol{n}, \tag{3}$$

where $\boldsymbol{l}$ is the unit vector at the intersection line and $\boldsymbol{n}$ is the normal vector of the GB plane shown in Fig. 5. The angle $\psi$ is between the intersection lines. The favored slip transfer is here the slip that minimizes the angles between the intersection lines and the slip directions [29]. Later, Shen et al. [17] concluded that emitted slip systems are successfully predicted if the geometric criterion (3) is accompanied by a criterion maximizing the resolved shear stress exerted on the emitted dislocations.

Moreover, the interaction between dislocations and grain boundaries were studied by Lee et al. [30, 31] based on in situ transmission electron microscope (TEM) deformation experiments, they proposed three criteria, the so-called Lee-Robertson-Birnbaum (LRB) criteria, determining which outgoing slip system will be probably activated during dislocation transmission. These criteria are introduced in the following, determining which outgoing slip system will be probably activated during dislocation transmission. These criteria are introduced in the following:

- First, a geometric condition is taken into account. It is to minimize the angle $\psi$ between the intersection lines.
- Second, maximizing the resolved shear stress (RSS factor) which acts on the outgoing slip system and is induced by the incoming piled-up dislocations.
- Third, minimizing the residual grain boundary dislocation determined by the difference between Burgers vectors of incoming and outgoing dislocations.

In the early stages of slip transfer, the first criterion identifies an active slip plane. Then the second and third criteria

determine active slip directions. Figure 4 in [15] details schematically the implementation of LRB criteria.

In the direction of formulating the slip transfer and force balances at a GB, a recent theory in the framework of strain gradient plasticity was proposed by Gurtin [113]. This GB theory accounts automatically for the grain misorientation and grain boundary orientation. As a key point in this theory, a GB free-energy as a function of GB Burgers vector production $\mathbb{G}$ was first proposed, $\mathbb{G}$ is given by:

$$\mathbb{G} = \sum_{\alpha} \left[\gamma_{\mathrm{B}}^{\alpha} \boldsymbol{s}_{\mathrm{B}}^{\alpha} \otimes \boldsymbol{m}_{\mathrm{B}}^{\alpha} - \gamma_{\mathrm{A}}^{\alpha} \boldsymbol{s}_{\mathrm{A}}^{\alpha} \otimes \boldsymbol{m}_{\mathrm{A}}^{\alpha}\right](\boldsymbol{n}\times),$$

$$|\mathbb{G}|^2 = \sum_{\alpha\beta} \left[\mathrm{C}_{\mathrm{AA}}^{\alpha\beta} \gamma_{\mathrm{A}}^{\alpha} \gamma_{\mathrm{A}}^{\beta} + \mathrm{C}_{\mathrm{BB}}^{\alpha\beta} \gamma_{\mathrm{B}}^{\alpha} \gamma_{\mathrm{B}}^{\beta} - 2\mathrm{C}_{\mathrm{AB}}^{\alpha\beta} \gamma_{\mathrm{A}}^{\alpha} \gamma_{\mathrm{B}}^{\beta}\right], \quad (4)$$

where A and B indicate adjacent grains to a GB and $\gamma$ is the slip flow. $\mathbb{G}$ is affected by intra- and inter-grains moduli given by:

$$\mathrm{C}_{\mathrm{IJ}}^{\alpha\beta} = \left(\boldsymbol{s}_{\mathrm{I}}^{\alpha} \cdot \boldsymbol{s}_{\mathrm{J}}^{\beta}\right)\left(\boldsymbol{m}_{\mathrm{I}}^{\alpha} \times \boldsymbol{n}\right) \cdot \left(\boldsymbol{m}_{\mathrm{J}}^{\beta} \times \boldsymbol{n}\right) \quad (5)$$

Here, the generic labels I and J are replaced by A and B, if $\mathrm{I} = \mathrm{J}$ denote the slip interaction intra-grains moduli and if $\mathrm{I} \neq \mathrm{J}$ represents the slip interaction inter-grain modulus which mimics Eq. (3). The resultant shear stresses acting on the slip systems as well as microforces induced by residual dislocations at the grain boundary are all related through a flow rule affected by inter- and intra-grain moduli.

Following the interaction modulus discussed in this section as well as the experimental works discussed in the previous sections, a numerical observation of the interaction between dislocation flows and GBs through nanoindentations applied at the area of a GB, is highly demanding in the field. In this regard, and referring to the continuum scale, strain gradient crystal plasticity frameworks with the potential of contributing a description of GNDs into traditional plasticity theories, are of high interest. These frameworks may provide an observation dislocation pile-up at GBs as well as a formulation of microforces acting at GBs. Moreover, in a combination of this framework with a GB theory such as the model proposed by Gurtin [113], the effects of geometric criteria, the role of shear stresses on the directional flows, and effects of residual burgers vectors at GBs are all taken into account.

To the best of authors' knowledge, there is no study of GB pop-in based on continuum theories in the literature. Although there is one three-dimensional simulation of nanoindentation tests [114] based on a strain gradient theory, where a flat punch is indented close to a GB, and the effects of low- and high-angle GBs on the external load–displacement data are captured and reported in Fig. 10 in [114]. It is worth highlighting that a conventional crystal plasticity theory along with a series of geometric slip criteria have been recently implemented in a MATLAB toolbox called STABIX [115]. By employing this toolbox, Su et al. [116] investigated the effect of grain boundaries on the topography of the indented area at a range of variation of $m'$ detailed in Eq. (2). Figure 9 in [116] compares the numerical and experimental observations. It was concluded that the difficulty in the slip transfer across GBs is pronounced at the GBs corresponding to poorly aligned slip systems and consequently, associated with the low values of $m'$.

Focusing on the smaller scales than the continuum level, a discrete dislocation study by Lu et al. [117] has recently investigated a bicrystal indented at the area of a GB. Figure 8 in [117] is reproduced here in Fig. 6 and shows two plateaus in the force data which are associated with displacement bursts at the order of 10% of burgers vector magnitude ($b = 0.25nm$) given in Table 1 in [117]. These relatively small plateaus in force–displacement data, were therein referred to as the effect of GB pop-in. Lu et al. [117] envisaged that performing this simulation in a larger dimension might pronounce the observations as seen in experiments. For the sake of completeness, it could be here mentioned that molecular dynamics simulations

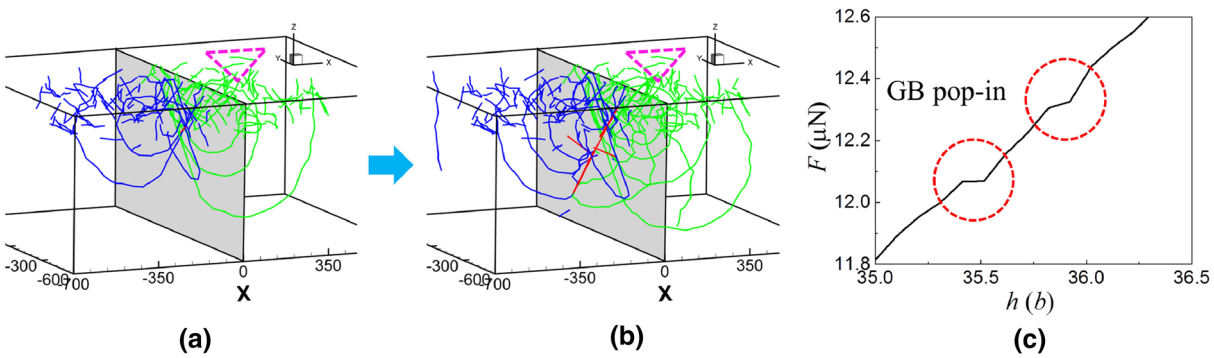


**Figure 6:** (a) Dislocation structure before penetration, (b) dislocation structure after penetration, and (c) load–displacement data around the moment of penetration. Adapted with permission from Ref. [117].

of nanoindentation in the vicinity of grain boundaries have also been endeavored in [118–120].

## Summary and conclusions

Grain boundaries play a paramount role in the deformation of polycrystalline materials, specifically dislocation–grain boundary interactions lead to different deformation mechanisms, which need to be studied in detail. Using nanoindentation, the localized plastic deformation in the plastic zone allows probing the individual grain boundary–dislocation interactions for a wide variety of grain boundaries and materials. In the present article, recent advances on dislocation–individual grain boundary interactions studied via nanoindentation testing are reviewed, which are mainly focused on the experimental studies on the occurrence of the GB pop-in events, localized GB movement under ambient conditions, and an analysis of the slip transfer mechanism using theoretical treatments and simulations.

The occurrence of the GB pop-in events on the LD curve is strongly influenced by the distance of the indenter from the GB, misorientation between the adjacent grains, GB character, and the applied load. The GB pop-in events are believed to be associated with the dislocations absorption at the GB and their re-emission in the adjacent grain. It is, however, unclear why the GB pop-in is experimentally mainly observed for BCC metals. One open question is related to the local stresses acting on the GB, causing the occurrence of such a yield event for the specific grain boundaries.

There is clear evidence, from the three-dimensional analysis of the dislocation structure just after the GB pop-in, that dislocations pile-up at the GB and are then transmitted in the adjacent grain [70]. Furthermore, localized GB movement on and below the residual impression in tungsten have been reported, which is not considered as a usual deformation phenomenon for refractory metals at room temperature [9]. This localized GB movement under ambient condition is believed to occur due to the inhomogeneous state of stresses during the nanoindentation. On the other hand, for GB pop-in events, the dislocation absorption at the GB and their re-emission in the adjacent grain is reported to be the possible mechanism. For the slip transfer mechanism, several criteria have been theoretically developed. However, further experimental effort is needed for a wide range of grain boundaries and deformation conditions. New computational approaches at various length and time scales are also required to understand the complex interaction between the plastic zone of an indentation and individual grain boundaries. The local mechanical response at the grain boundary pop-in is thought to be an important parameter, which together with simulations will help to further understand the complex GB yield phenomena.

## Acknowledgments

H.P. and K.D. acknowledge the support by the German Research Foundation (DFG) for research grant Po_ 2242/3-1 and Du 424/16-1.

## Funding

Open Access funding enabled and organized by Projekt DEAL.

## Data availability

Data will be made available on reasonable request.

## Compliance with ethical standards

**Conflict of interest** On behalf of all authors, the corresponding author states that there is no conflict of interest.



## References

1. J.P. Hirth, The influence of grain boundaries on mechanical properties. Metall. Trans. **3**(12), 3047 (1972)
2. E.O. Hall, The deformation and ageing of mild steel. II. Characteristics of the Lüders deformation. Proc. Phys. Soc. Sect. B **64**(9), 742 (1951)
3. S. Kondo, T. Mitsuma, N. Shibata, Y. Ikuhara, Direct observation of individual dislocation interaction processes with grain boundaries. Sci. Adv. **2**(11), e1501926 (2016)
4. S.J. Fensin, S.M. Valone, E.K. Cerreta, G.T. Gray, Influence of grain boundary properties on spall strength: grain boundary energy and excess volume. J. Appl. Phys. **112**(8), 083529 (2012)
5. A. Ma, F. Roters, D. Raabe, On the consideration of interactions between dislocations and grain boundaries in crystal plasticity

finite element modeling—theory, experiments, and simulations. Acta Mater. **54**(8), 2181 (2006)
6. P.R.M. Van Beers, V.G. Kouznetsova, M.G.D. Geers, M.A. Tschopp, D.L. McDowell, A multiscale model of grain boundary structure and energy: From atomistics to a continuum description. Acta Mater. **82**, 513 (2015)
7. S. Chen, Q. Yu, The role of low angle grain boundary in deformation of titanium and its size effect. Scr. Mater. **163**, 148 (2019)
8. M. Stricker, J. Gagel, S. Schmitt, K. Schulz, D. Weygand, P. Gumbsch, On slip transmission and grain boundary yielding. Meccanica **51**(2), 271 (2016)
9. F. Javaid, K. Durst, Stress-driven grain boundary movement during nanoindentation in tungsten at room temperature. Materialia **1**, 99 (2018)
10. M. Hamid, H. Lyu, B.J. Schuessler, P.C. Wo, H.M. Zbib, modeling and characterization of grain boundaries and slip transmission in dislocation density-based crystal plasticity. Crystals **7**(6), 152 (2017)
11. P.J. Imrich, C. Kirchlechner, C. Motz, G. Dehm, Differences in deformation behavior of bicrystalline Cu micropillars containing a twin boundary or a large-angle grain boundary. Acta Mater. **73**, 240 (2014)
12. J.R. Greer, J.T.M. De Hosson, Plasticity in small-sized metallic systems: Intrinsic versus extrinsic size effect. Prog. Mater. Sci. **56**(6), 654 (2011)
13. N. Kheradmand, H. Vehoff, Orientation gradients at boundaries in micron-sized bicrystals. Adv. Eng. Mater. **14**(3), 153 (2012)
14. J. Kacher, B.P. Eftink, B. Cui, I.M. Robertson, Dislocation interactions with grain boundaries. Curr. Opin. Solid State Mater. Sci. **18**(4), 227 (2014)
15. E. Bayerschen, A.T. McBride, B.D. Reddy, T. Böhlke, Review on slip transmission criteria in experiments and crystal plasticity models. J. Mater. Sci. **51**(5), 2243 (2016)
16. L.C. Lim, R. Raj, Continuity of slip screw and mixed crystal dislocations across bicrystals of nickel at 573 K. Acta Metall. **33**(8), 1577 (1985)
17. Z. Shen, R.H. Wagoner, W.A.T. Clark, Dislocation and grain boundary interactions in metals. Acta Metall. **36**(12), 3231 (1988)
18. S. Zghal, A. Couret, Transmission of the deformation through γ-γ interfaces in a polysynthetically twinned TiAl alloy II. Twin interfaces (180° rotational). Philos. Mag. A Phys. Condens. Matter, Struct. Defects Mech. Prop. **81**(2), 365 (2001)
19. A. Gemperle, N. Zárubová, J. Gemperlová, Reactions of slip dislocations with twin boundary in Fe-Si bicrystals. J. Mater. Sci. **40**(12), 3247 (2005)
20. R.C. Pond, D.L. Medlin, A. Serra, A study of the accommodation of coherency strain by interfacial defects at a grain boundary in gold. Philos. Mag. **86**(29–31), 4667 (2006)
21. M.P. Miller, P.R. Dawson, Understanding local deformation in metallic polycrystals using high energy X-rays and finite elements. Curr. Opin. Solid State Mater. Sci. **18**(5), 286 (2014)
22. H. Pouriayevali, B.-X. Xu, Decomposition of dislocation densities at grain boundary in a finite-deformation gradient crystal-plasticity framework. Int. J. Plasticity **96**, 36 (2017)
23. I. Özdemir, T. Yalçinkaya, Modeling of dislocation-grain boundary interactions in a strain gradient crystal plasticity framework. Comput. Mech. **54**(2), 255 (2014)
24. D.E. Spearot, M.D. Sangid, Insights on slip transmission at grain boundaries from atomistic simulations. Curr. Opin. Solid State Mater. Sci. **18**(4), 188 (2014)
25. L. Zhang, C. Lu, K. Tieu, A review on atomistic simulation of grain boundary behaviors in face-centered cubic metals. Comput. Mater. Sci. **118**, 180 (2016)
26. B. Liu, P. Eisenlohr, F. Roters, D. Raabe, Simulation of dislocation penetration through a general low-angle grain boundary. Acta Mater. **60**(13–14), 5380 (2012)
27. S. Xu, L. Xiong, Y. Chen, D.L. McDowell, Sequential slip transfer of mixed-character dislocations across Σ3 coherent twin boundary in FCC metals: a concurrent atomistic-continuum study. NPJ Comput. Mater. **2**(1), 15016 (2016)
28. J.D. Livingston, B. Chalmers, Multiple slip in bicrystal deformation. Acta Metall. **5**(6), 322 (1957)
29. Z. Shen, R.H. Wagoner, W.A.T. Clark, Dislocation pile-up and grain boundary interactions in 304 stainless steel. Scr. Metall. **20**(6), 921 (1986)
30. T.C. Lee, I.M. Robertson, H.K. Birnbaum, Prediction of slip transfer mechanisms across grain boundaries. Scr. Metall. **23**(5), 799 (1989)
31. T.C. Lee, I.M. Robertson, H.K. Birnbaum, AnIn Situ transmission electron microscope deformation study of the slip transfer mechanisms in metals. Metall. Trans. A **21**(9), 2437 (1990)
32. S. Wulfinghoff, E. Bayerschen, T. Böhlke, A gradient plasticity grain boundary yield theory. Int. J. Plasticity **51**, 33 (2013)
33. S. Bargmann, M. Ekh, K. Runesson, B. Svendsen, Modeling of polycrystals with gradient crystal plasticity: a comparison of strategies. Philos. Mag. **90**(10), 1263 (2010)
34. C.J. Bayley, W.A.M. Brekelmans, M.G.D. Geers, A three-dimensional dislocation field crystal plasticity approach applied to miniaturized structures. Philos. Mag. **87**(8–9), 1361 (2007)
35. A. Ma, F. Roters, D. Raabe, A dislocation density based constitutive model for crystal plasticity FEM including geometrically necessary dislocations. Acta Mater. **54**(8), 2169 (2006)
36. Z. Budrovic, Plastic deformation with reversible peak broadening in nanocrystalline nickel. Science (80–) **304**(5668), 273 (2004)
37. S. Van Petegem, L. Li, P.M. Anderson, H. Van Swygenhoven, Deformation mechanisms in nanocrystalline metals: insights

from in-situ diffraction and crystal plasticity modelling. Thin Solid Films **530**, 20 (2013)
38. H. Van Swygenhoven, S. Van Petegem, In-situ mechanical testing during X-ray diffraction. Mater. Charact. **78**, 47 (2013)
39. E.A. West, G.S. Was, Strain incompatibilities and their role in intergranular cracking of irradiated 316L stainless steel. J. Nucl. Mater. **441**(1–3), 623 (2013)
40. M.A. Haque, M.T.A. Saif, In-situ tensile testing of nano-scale specimens in SEM and TEM. Exp. Mech. **42**(1), 123 (2002)
41. D. Zhang, J.M. Breguet, R. Clavel, L. Phillippe, I. Utke, J. Michler, In situ tensile testing of individual Co nanowires inside a scanning electron microscope. Nanotechnology **20**(36), 365706 (2009)
42. M.B.H. Slama, N. Maloufi, J. Guyon, S. Bahi, L. Weiss, A. Guitton, In situ macroscopic tensile testing in SEM and electron channeling contrast imaging: pencil glide evidenced in a bulk β-Ti21S polycrystal. Materials (Basel). **12**(15), 2479 (2019)
43. M.D. McMurtrey, G.S. Was, B. Cui, I. Robertson, L. Smith, D. Farkas, Strain localization at dislocation channel-grain boundary intersections in irradiated stainless steel. Int. J. Plasticity **56**, 219 (2014)
44. L. Patriarca, W. Abuzaid, H. Sehitoglu, H.J. Maier, Slip transmission in bcc FeCr polycrystal. Mater. Sci. Eng. A **588**, 308 (2013)
45. W.Z. Abuzaid, M.D. Sangid, J.D. Carroll, H. Sehitoglu, J. Lambros, Slip transfer and plastic strain accumulation across grain boundaries in Hastelloy X. J. Mech. Phys. Solids **60**(6), 1201 (2012)
46. A.J. Wilkinson, E.E. Clarke, T.B. Britton, P. Littlewood, P.S. Karamched, High-resolution electron backscatter diffraction: an emerging tool for studying local deformation. J. Strain Anal. Eng. Des. **45**(5), 365 (2010)
47. L. Wang, Y. Yang, P. Eisenlohr, T.R. Bieler, M.A. Crimp, D.E. Mason, Twin nucleation by slip transfer across grain boundaries in commercial purity titanium. Metall. Mater. Trans. A Phys. Metall. Mater. Sci. **41**(2), 421 (2010)
48. C. Zambaldi, D. Raabe, Plastic anisotropy of γ-TiAl revealed by axisymmetric indentation. Acta Mater. **58**(9), 3516 (2010)
49. L. Wang, J. Teng, P. Liu, A. Hirata, E. Ma, Z. Zhang, M. Chen, X. Han, Grain rotation mediated by grain boundary dislocations in nanocrystalline platinum. Nat. Commun. **5**, 1 (2014)
50. Z. Zhang, É. Ódor, D. Farkas, B. Jóni, G. Ribárik, G. Tichy, S.H. Nandam, J. Ivanisenko, M. Preuss, T. Ungár, Dislocations in grain boundary regions: the origin of heterogeneous microstrains in nanocrystalline materials. Metall. Mater. Trans. A Phys. Metall. Mater. Sci. **51**(1), 513 (2020)
51. Q. Lin, X. An, H. Liu, Q. Tang, P. Dai, X. Liao, In-situ high-resolution transmission electron microscopy investigation of grain boundary dislocation activities in a nanocrystalline CrMnFeCoNi high-entropy alloy. J. Alloys Compd. **709**, 802 (2017)
52. G. Dehm, Miniaturized single-crystalline fcc metals deformed in tension: new insights in size-dependent plasticity. Prog. Mater. Sci. **54**(6), 664 (2009)
53. M.D. Uchic, D.M. Dimiduk, A methodology to investigate size scale effects in crystalline plasticity using uniaxial compression testing. Mater. Sci. Eng. A **400–401**(1–2 SUPPL.), 268 (2005)
54. A. Kunz, S. Pathak, J.R. Greer, Size effects in Al nanopillars: single crystalline vs. bicrystalline. Acta Mater. **59**(11), 4416 (2011)
55. C.A. Volkert, E.T. Lilleodden, Size effects in the deformation of sub-micron Au columns. Philos. Mag. **86**(33–35), 5567 (2006)
56. R. Soler, J.M. Molina-Aldareguia, J. Segurado, J. Llorca, R.I. Merino, V.M. Orera, Micropillar compression of LiF [111] single crystals: effect of size, ion irradiation and misorientation. Int. J. Plasticity **36**, 50 (2012)
57. M.D. Uchic, P.A. Shade, D.M. Dimiduk, Plasticity of micrometer-scale single crystals in compression. Annu. Rev. Mater. Res. **39**, 361 (2009)
58. K.S. Ng, A.H.W. Ngan, Deformation of micron-sized aluminium bi-crystal pillars. Philos. Mag. **89**(33), 3013 (2009)
59. N. Takata, S. Takeyasu, H. Li, A. Suzuki, M. Kobashi, Anomalous size-dependent strength in micropillar compression deformation of commercial-purity aluminum single-crystals. Mater. Sci. Eng. A **772**, 138710 (2020)
60. W. Ludwig, J.Y. Buffière, S. Savelli, P. Cloetens, Study of the interaction of a short fatigue crack with grain boundaries in a cast Al alloy using X-ray microtomography. Acta Mater. **51**(3), 585 (2003)
61. N. Kheradmand, J. Dake, A. Barnoush, H. Vehoff, Novel methods for micromechanical examination of hydrogen and grain boundary effects on dislocations. Philos. Mag. **92**(25–27), 3216 (2012)
62. J.S. Weaver, N. Li, N.A. Mara, D.R. Jones, H. Cho, C.A. Bronkhorst, S.J. Fensin, G.T. Gray, Slip transmission of high angle grain boundaries in body-centered cubic metals: micropillar compression of pure Ta single and bi-crystals. Acta Mater. **156**, 356 (2018)
63. C. Minnert, W.C. Oliver, K. Durst, New ultra-high temperature nanoindentation system for operating at up to 1100 °C. Mater. Des. **192**, 108727 (2020)
64. K. Durst, V. Maier, Dynamic nanoindentation testing for studying thermally activated processes from single to nanocrystalline metals. Curr. Opin. Solid State Mater. Sci. **19**(6), 340 (2015)
65. V. Maier, K. Durst, J. Mueller, B. Backes, H.W. Höppel, M. Göken, Nanoindentation strain-rate jump tests for determining the local strain-rate sensitivity in nanocrystalline Ni and ultrafine-grained Al. J. Mater. Res. **26**(11), 1421 (2011)
66. P.S. Phani, W.C. Oliver, G.M. Pharr, Understanding and modeling plasticity error during nanoindentation with continuous stiffness measurement. Mater. Des. **194**, 108923 (2020)

67. M.G. Wang, A.H.W. Ngan, Indentation strain burst phenomenon induced by grain boundaries in niobium. J. Mater. Res. **19**(8), 2478 (2004)
68. T.B.B. Britton, D. Randman, A.J. Wilkinson, Nanoindentation study of slip transfer phenomenon at grain boundaries. J. Mater. Res. **24**(03), 607 (2009)
69. W.A. Soer, J.T.M. De Hosson, Detection of grain-boundary resistance to slip transfer using nanoindentation. Mater. Lett. **59**(24–25), 3192 (2005)
70. F. Javaid, Y. Xu, K. Durst, Local analysis on dislocation structure and hardening during grain boundary pop-ins in tungsten. J. Mater. Sci. **55**(22), 9597 (2020)
71. L. Chang, L. Zhang, Mechanical behaviour characterisation of silicon and effect of loading rate on pop-in: a nanoindentation study under ultra-low loads. Mater. Sci. Eng. A **506**(1–2), 125 (2009)
72. T.-H. Ahn, C.-S. Oh, D.H. Kim, K.H. Oh, H. Bei, E.P. George, H.N. Han, Investigation of strain-induced martensitic transformation in metastable austenite using nanoindentation. Scr. Mater. **63**(5), 540 (2010)
73. N. de la Rosa-Fox, V. Morales-Flórez, J.A. Toledo-Fernández, M. Piñero, R. Mendoza-Serna, L. Esquivias, Nanoindentation on hybrid organic/inorganic silica aerogels. J. Eur. Ceram. Soc. **27**(11), 3311 (2007)
74. F. Javaid, E. Bruder, K. Durst, Indentation size effect and dislocation structure evolution in (001) oriented $SrTiO_3$ Berkovich indentations: HR-EBSD and etch-pit analysis. Acta Mater. **139**, 1 (2017)
75. F. Javaid, K.E. Johanns, E.A. Patterson, K. Durst, Temperature dependence of indentation size effect, dislocation pile-ups, and lattice friction in (001) strontium titanate. J. Am. Ceram. Soc. **101**(1), 356 (2018)
76. F. Javaid, A. Stukowski, K. Durst, 3D Dislocation structure evolution in strontium titanate: Spherical indentation experiments and MD simulations. J. Am. Ceram. Soc. **100**(3), 1134 (2017)
77. W.D. Nix, H. Gao, Indentation size effects in crystalline materials: a law for strain gradient plasticity. J. Mech. Phys. Solids **46**(3), 411 (1998)
78. K. Durst, B. Backes, M. Göken, Indentation size effect in metallic materials: correcting for the size of the plastic zone. Scr. Mater. **52**(11), 1093 (2005)
79. A. Montagne, V. Audurier, C. Tromas, Influence of pre-existing dislocations on the pop-in phenomenon during nanoindentation in MgO. Acta Mater. **61**(13), 4778 (2013)
80. P. Sadrabadi, K. Durst, M. Göken, Study on the indentation size effect in $CaF_2$: dislocation structure and hardness. Acta Mater. **57**(4), 1281 (2009)
81. F. Javaid, Y. Xu, E. Bruder, K. Durst, Indentation size effect in tungsten: quantification of geometrically necessary dislocations underneath the indentations using HR-EBSD. Mater. Charact. **142**, 39–42 (2018)
82. S. Jakob, A. Leitner, A. Lorich, M. Eidenberger-Schober, W. Knabl, R. Pippan, H. Clemens, V. Maier-Kiener, Influence of crystal orientation and Berkovich tip rotation on the mechanical characterization of grain boundaries in molybdenum. Mater. Des. **182**, 107998 (2019)
83. A.M. Minor, E.T. Lilleodden, E.A. Stach, J.W. Morris, Direct observations of incipient plasticity during nanoindentation of Al. J. Mater. Res. **19**(01), 176 (2004)
84. Y. Gaillard, C. Tromas, J. Woirgard, Pop-in phenomenon in MgO and LiF: observation of dislocation structures. Philos. Mag. Lett. **83**(9), 553 (2003)
85. K.J. Van Vliet, J. Li, T. Zhu, S. Yip, S. Suresh, Quantifying the early stages of plasticity through nanoscale experiments and simulations. Phys. Rev. B Condens. Matter Mater. Phys. **67**(10), 104105 (2003)
86. L. Zhang, T. Ohmura, Plasticity initiation and evolution during nanoindentation of an iron-3% silicon crystal. Phys. Rev. Lett. **112**(14), 1 (2014)
87. S. Shim, H. Bei, E.P. George, G.M. Pharr, A different type of indentation size effect. Scr. Mater. **59**(10), 1095 (2008)
88. T. Ohmura, K. Tsuzaki, F. Yin, Nanoindentation-induced deformation behavior in the vicinity of single grain boundary of interstitial-free steel. Mater. Trans. **46**(9), 2026 (2005)
89. W.A. Soer, K.E. Aifantis, J.T.M. De Hosson, Incipient plasticity during nanoindentation at grain boundaries in body-centered cubic metals. Acta Mater. **53**(17), 4665 (2005)
90. K.E. Aifantis, W.A. Soer, J.T.M. De Hosson, J.R. Willis, Interfaces within strain gradient plasticity: theory and experiments. Acta Mater. **54**(19), 5077 (2006)
91. T. Eliash, M. Kazakevich, V.N. Semenov, E. Rabkin, Nanohardness of molybdenum in the vicinity of grain boundaries and triple junctions. Acta Mater. **56**(19), 5640 (2008)
92. P.C. Wo, A.H.W. Ngan, Investigation of slip transmission behavior across grain boundaries in polycrystalline $Ni_3Al$ using nanoindentation. J. Mater. Res. **19**(01), 189 (2004)
93. B. Lagow, I. Robertson, M. Jouiad, D. Lassila, T. Lee, H. Birnbaum, Observation of dislocation dynamics in the electron microscope. Mater. Sci. Eng. A **309–310**, 445 (2001)
94. D. Faghihi, G.Z. Voyiadjis, Determination of nanoindentation size effects and variable material intrinsic length scale for body-centered cubic metals. Mech. Mater. **44**, 189 (2012)
95. F. Javaid, Indentation size effect: analysis of underlying mechanisms in (001) oriented strontium titanate single crystal via chemical etching and EBSD. PhD Thesis (2017). https://tuprints.ulb.tu-darmstadt.de/6762/
96. M. Jin, A.M. Minor, E.A. Stach, J.W. Morris, Direct observation of deformation-induced grain growth during the nanoindentation of ultrafine-grained Al at room temperature. Acta Mater. **52**(18), 5381 (2004)
97. M. Jin, A.M. Minor, J.W. Morris, Strain-induced coarsening in nano-grained films. Thin Solid Films **515**(6), 3202 (2007)

98. K. Zhang, J.R. Weertman, J.A. Eastman, Rapid stress-driven grain coarsening in nanocrystalline Cu at ambient and cryogenic temperatures. Appl. Phys. Lett. **87**(6), 1 (2005)
99. T.J. Rupert, D.S. Gianola, Y. Gan, K.J. Hemker, Experimental observations of stress-driven grain boundary migration. Science **326**(December), 1686 (2009)
100. M. Legros, D.S. Gianola, K.J. Hemker, In situ TEM observations of fast grain-boundary motion in stressed nanocrystalline aluminum films. Acta Mater. **56**(14), 3380 (2008)
101. D.S. Gianola, D.H. Warner, J.F. Molinari, K.J. Hemker, Increased strain rate sensitivity due to stress-coupled grain growth in nanocrystalline Al. Scr. Mater. **55**(7), 649 (2006)
102. D. Pan, S. Kuwano, T. Fujita, M.W. Chen, Ultra-large room-temperature compressive plasticity of a nanocrystalline metal. Nano Lett. **7**(7), 2108 (2007)
103. D.S. Gianola, S. Van Petegem, M. Legros, S. Brandstetter, H. Van Swygenhoven, K.J. Hemker, Stress-assisted discontinuous grain growth and its effect on the deformation behavior of nanocrystalline aluminum thin films. Acta Mater. **54**(8), 2253 (2006)
104. W.A. Soer, J.T.M. De Hosson, A.M. Minor, J.W. Morris, E.A. Stach, Effects of solute Mg on grain boundary and dislocation dynamics during nanoindentation of Al-Mg thin films. Acta Mater. **52**(20), 5783 (2004)
105. J.W. Cahn, J.E. Taylor, A unified approach to motion of grain boundaries, relative tangential translation along grain boundaries, and grain rotation. Acta Mater. **52**(16), 4887 (2004)
106. J.W. Cahn, Y. Mishin, A. Suzuki, Coupling grain boundary motion to shear deformation. Acta Mater. **54**(19), 4953 (2006)
107. M. Winning, G. Gottstein, L.S. Shvindlerman, Stress induced grain boundary motion. Acta Mater. **49**(2), 211 (2001)
108. M. Winning, G. Gottstein, L.S. Shvindlerman, On the mechanisms of grain boundary migration. Acta Mater. **50**(2), 353 (2002)
109. V.A. Ivanov, Y. Mishin, Dynamics of grain boundary motion coupled to shear deformation: an analytical model and its verification by molecular dynamics. Phys. Rev. B Condens. Matter Mater. Phys. **78**(6), 1 (2008)
110. J. Luster, M.A. Morris, Compatibility of deformation in two-phase Ti-Al alloys: dependence on microstructure and orientation relationships. Metall. Mater. Trans. A **26**(7), 1745 (1995)
111. T.R. Bieler, R. Alizadeh, M. Peña-Ortega, J. Llorca, An analysis of (the lack of) slip transfer between near-cube oriented grains in pure Al. Int. J. Plasticity **118**, 269 (2019)
112. S. Hémery, P. Nizou, P. Villechaise, In situ SEM investigation of slip transfer in Ti-6Al-4V: Effect of applied stress. Mater. Sci. Eng. A **709**, 277 (2018)
113. M.E. Gurtin, A theory of grain boundaries that accounts automatically for grain misorientation and grain-boundary orientation. J. Mech. Phys. Solids **56**(2), 640 (2008)
114. A.T. McBride, D. Gottschalk, B.D. Reddy, P. Wriggers, A. Javili, Computational and theoretical aspects of a grain-boundary model at finite deformations. Tech. Mech. **36**(1–2), 102 (2016)
115. D. Mercier, C. Zambaldi, T.R. Bieler, STABiX Documentation. September 2015
116. Y. Su, C. Zambaldi, D. Mercier, P. Eisenlohr, T.R. Bieler, M.A. Crimp, Quantifying deformation processes near grain boundaries in α titanium using nanoindentation and crystal plasticity modeling. Int. J. Plasticity **86**, 170 (2016)
117. S. Lu, B. Zhang, X. Li, J. Zhao, M. Zaiser, H. Fan, X. Zhang, Grain boundary effect on nanoindentation: a multiscale discrete dislocation dynamics model. J. Mech. Phys. Solids **126**, 117 (2019)
118. S.W. Liang, R.Z. Qiu, T.H. Fang, Molecular dynamics simulations of nanoindentation and scratch in Cu grain boundaries. Beilstein J. Nanotechnol. **8**(1), 2283 (2017)
119. X. Liu, F. Yuan, Y. Wei, Grain size effect on the hardness of nanocrystal measured by the nanosize indenter. Appl. Surf. Sci. **279**, 159 (2013)
120. C. Huang, X. Peng, T. Fu, X. Chen, H. Xiang, Q. Li, N. Hu, Molecular dynamics simulation of BCC Ta with coherent twin boundaries under nanoindentation. Mater. Sci. Eng. A **700**, 609 (2017)